

CHAPTER 4

SPECTRAL MIXTURE ANALYSIS OF LANDSAT THEMATIC MAPPER IMAGES APPLIED TO THE DETECTION OF THE TRANSIENT SNOWLINE ON TROPICAL ANDEAN GLACIERS

Abstract

The tropical glaciers in the central Andes are sensitive indicators of climatic change and provide an important water resource, but are presently in a state of rapid retreat. Spectral mixture analysis using Landsat Thematic Mapper (TM) images was found to provide robust identification of the ablation and accumulation zones at two tropical sites: Zongo Glacier in the Cordillera Real, Bolivia, and the Quelccaya Ice Cap in Peru. Delineation of the accumulation and ablation zones is relatively insensitive to the endmembers selected to represent each zone. Endmembers selected from Zongo Glacier were used with equal success on the Quelccaya Ice Cap. Spectral mixture analysis was found to be superior to the use of single band images or the TM4/TM5 ratio in discriminating the accumulation zones on these small tropical glaciers. The position of the transient snowline identified on Zongo Glacier is consistent with the elevation of the equilibrium line determined from mass balance studies. This suggests that as in mid-latitudes, the elevation of the transient snowline on tropical glaciers at the end of the ablation season is a good proxy for the elevation of the equilibrium line.

Introduction

Tropical glaciers are extremely sensitive, but complex, indicators of climatic change (Hastenrath, 1984b), yet have received very little attention compared to their mid-latitude counterparts. Although tropical glaciers have been in a state of retreat since the 19th century (Hastenrath, 1984b), determining the climatic causes responsible for the retreat is difficult because a glacier's response is affected by a host of climatic and non-climatic factors (Kerr, 1993). For instance, the observed retreat of the best-studied glacier in the tropics, Lewis Glacier, Mt. Kenya, appears to be caused in part by an increase in atmospheric humidity (Hastenrath and Kruss, 1992a; Hastenrath and Kruss, 1992b).

The primary method for relating glacier fluctuations to climatic changes is to measure directly the mass balance of a glacier over time. This is usually accomplished by monitoring ice gain or loss at a network of stakes covering the glacier surface or by photogrammetric surveys (Paterson, 1994; Williams *et al.*, 1991). However, such field programs are difficult and expensive; hence mass balance programs have been undertaken at only a few tropical locales. In fact, the only long term tropical mass balance study is on Lewis Glacier, Mt. Kenya, (Hastenrath, 1984a; Hastenrath, 1989). Shorter-term mass studies exist for glaciers in Irian Jaya (Hope *et al.*, 1976), the Cordillera Blanca of Peru (Hastenrath and Ames, 1995; Kaser *et al.*, 1990), and the Cordillera Real of Bolivia (Francou *et al.*, 1995; Ribstein *et al.*, 1995). Although additional studies are planned, the mass balance of only a handful

of the thousands of tropical glaciers will ever be measured directly. These detailed mass balance studies provide valuable knowledge of the response of tropical glaciers to climatic changes, but do not provide information about how local climatic and topography may differentially influence glaciers within a region.

Satellite remote sensing affords the potential to complement mass balance studies with inferences about relative changes in many additional tropical glaciers by monitoring the elevation of the transient snowline, which is defined as the lower limit of last year's snow (Østrem, 1975). For mid-latitude glaciers, and at least some tropical glaciers (B. Francou, personal communication), the elevation of the transient snowline at the end of the ablation season is approximately coincident with the equilibrium line altitude (ELA). The ELA is the elevation on a glacier where the mass balance is 0 (i.e. there is no net mass gain or loss during the balance year). Its elevation is inversely related to the annual net balance of the glacier. The more positive the net balance of a glacier, the lower the ELA, and the more negative a mass balance the higher the ELA. In fact, the height of the ELA has been found to be linearly correlated to the specific mass balance of several Norwegian glaciers (Østrem, 1975). Thus, by monitoring the transient snowline via satellite remote sensing, relative changes in mass balance of many glaciers within a region can be observed.

Remote sensing of the transient snowline

In the visible and near-infrared wavelengths, the transient snowline often appears as a sharp discontinuity in spectral albedo that separates the accumulation from the ablation zone (Paterson, 1994). In the accumulation zone, the glacier's surface is characterized by high reflectance snow or firn, whereas lower reflectance bare ice is exposed within the ablation zone. Using this spectral difference, visible and infrared satellite remote sensing has been successfully used to map the transient snowline since the beginning of the Landsat era in the early 1970s (Krimmel and Meier, 1975; Meier, 1973; Østrem, 1975). Subsequently, both Landsat Multispectral Scanner (MSS) and Landsat Thematic Mapper (TM) images have been used in numerous glaciological applications, such as mapping temporal changes in terminus position (e.g. Hall *et al.*, 1995a), delineation of snow and ice facies (e.g. Bayr *et al.*, 1994; Williams *et al.*, 1991), and determination of glacial albedo (Hall *et al.*, 1990; Hall *et al.*, 1989). However, with the exception of recent work measuring the retreat of glaciers in Irian Jaya using SPOT images (van Ufford and Sedgwick, submitted), satellite remote sensing of tropical glaciers has been limited.

Early work demonstrated that at least two spectrally distinct zones can be discriminated on many valley glaciers (Williams *et al.*, 1991). It is possible to distinguish these zones using individual bands within the visible and near-infrared portion of the spectrum, usually MSS7 (0.8-0.11 μm) or Landsat TM4 (0.76-0.90 μm). Additionally, the band ratio TM4/TM5 has

been commonly employed to delineate spectrally similar areas of the glacier and to distinguish the ablation zone from adjacent moraines (Bayr *et al.*, 1994; Hall *et al.*, 1987). Fresh snowfall and other environmental contaminants, soot, tephra, or rockfalls can obscure glacial boundaries (Hall *et al.*, 1987; Williams *et al.*, 1991).

Both single band images and band ratios have proven successful in delineating the accumulation and ablation areas of glaciers in mid-latitude regions, however, they are less reliable in tropical settings. The use of Landsat TM for glaciological studies is hampered by the saturation of the TM sensor in the first 3 bands, and occasionally band 4, over the accumulation areas, as well as the small size of tropical glaciers. Large differences in at-satellite reflectance occur on tropical glaciers due to varying slope orientations and shading from obscuring topography. Because of the limitations encountered with the previously employed methodologies, spectral mixture analysis was investigated as a tool for providing robust delineation of the transient snowline over large areas.

Spectral Mixture Analysis

Spectral mixture analysis provides a quantitative strategy for studying multispectral images (Adams and Smith, 1986). It has been successfully used in a wide variety of environmental applications including estimation of the fraction of an individual pixel covered with snow (Rosenthal and Dozier, 1996). In this study, estimation of the percentage of individual pixels

covered by a certain surface type was not the goal; rather spectral mixing was used to delineate the accumulation and ablation zones.

In spectral mixture analysis the reflectance of a pixel in an individual band is mathematically modeled as a linear or nonlinear sum of the reflectances of a small number of known components called endmembers. Linear mixing is an appropriate model if different surface materials are spatially separated within a pixel. In this case, a photon will interact with only a single surface material and the spectral mixture can be considered macroscopic. In intimate mixtures, however, photons interact with more than a single component and nonlinear mixing may occur (Sabol *et al.*, 1990). Possible sources of nonlinear effects on a glacier or snow-covered surface include absorption at visible and near-infrared wavelengths by contaminants or absorption in the shortwave infrared wavelengths by ice. Despite potential nonlinear effects, linear mixing has been shown appropriate for mapping montane snowcover (Rosenthal and Dozier, 1996).

In linear mixing the measured reflectance from an individual pixel in a single band is modeled as:

$$R_{measured,b} = \sum_{em=1}^N (F_{em,b} R_{em,b}) + \mathbf{e}_b \quad (1)$$

Where $R_{measured,b}$ is the measured reflectance in each band (b), $R_{em,b}$ is the reflectance of endmember, F_{em} is the fraction of each pixel covered by each endmember in each band (b). \mathbf{e}_b represents the error between the modeled

and measured reflectance in each band, and N is the total number of endmembers. Additionally, the sum of all endmember fractions is assumed to be unity:

$$\sum_{em=1}^N F_{em} = 1 \quad (2)$$

As the aim of the study was not a quantitative assessment of percentage of each pixel occupied by an individual endmember, endmember fractions were not constrained to be nonnegative. A root-mean-square (RMS) error was computed for each pixel based on the difference between the modeled and measured reflectance of each pixel in each band as:

$$e = \left[\frac{1}{n} \sum_1^n (R_{measured} - R_{modeled})^2 \right]^{1/2} \quad (3)$$

where n represents the number of bands.

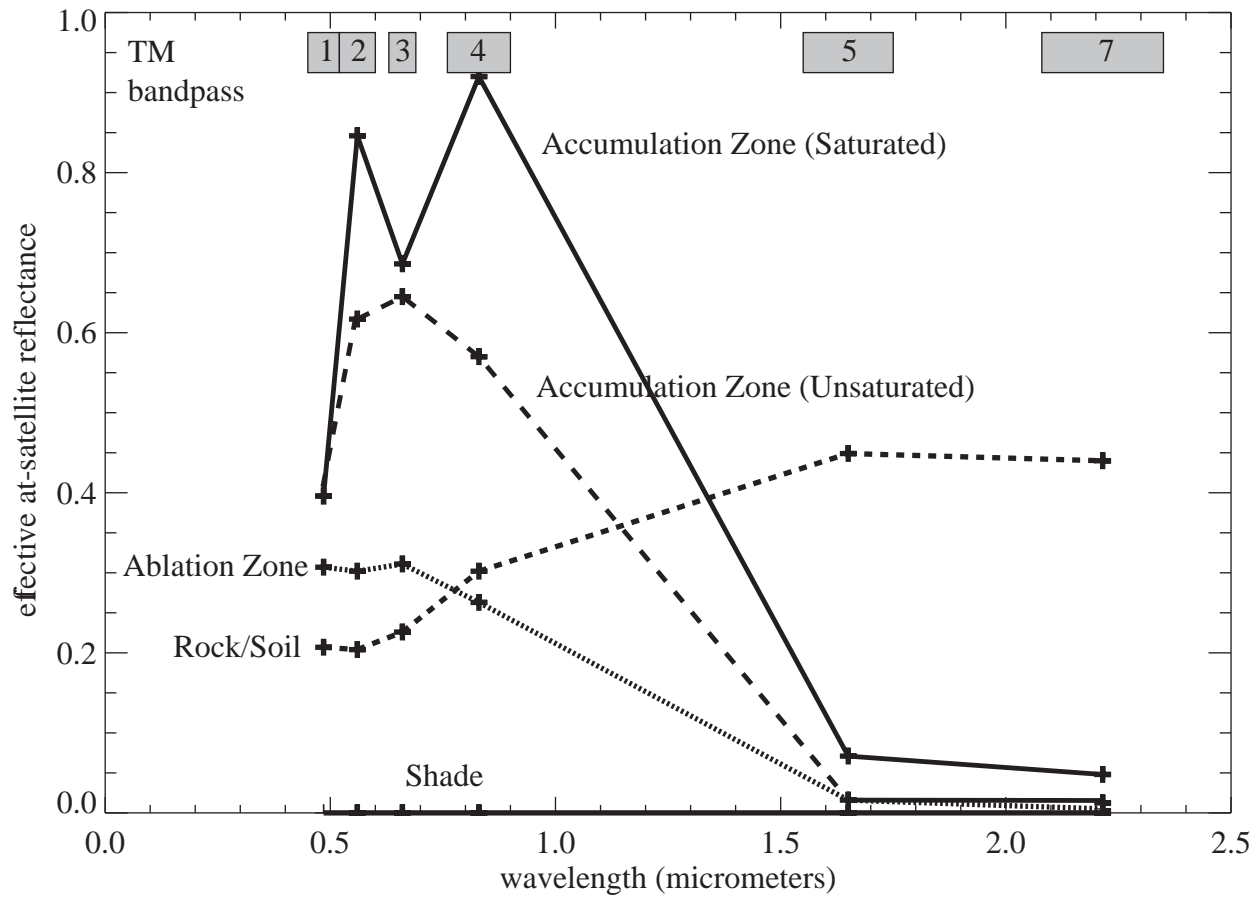
Determining the endmember fractions for each pixel requires solving equation (1) for each of the n bands and equation (2) simultaneously. The problem is overdetermined as there are more equations than unknowns. It is solved by finding a solution that best satisfies all equations simultaneously. This was accomplished by using a singular value decomposition (SVD) algorithm of Press *et al.* (1988) to invert the spectral endmembers and to determine the endmember fractions (Boardman, 1990). SVD was chosen because of its ability to solve singular or nearly singular equations, but it has the disadvantage of being computationally intensive.

Image Processing and Analysis

Two Landsat TM images , path 001 row 71 (ID 51249-14004: acquired August 2, 1987) and path 003 row 70 (ID 50511-14165: acquired July 25, 1985) were used to demonstrate the utility of spectral mixture analysis for detecting the transient snowline. Both were acquired in the middle of the dry season and the transient snowline may not yet have attained its highest annual altitude. However, this does not limit their usefulness in assessing the performance of spectral mixture analysis. Prior to performing spectral unmixing, the original TM digital values were converted to at-satellite reflectance using the procedure described in Markum and Barker (1986) and a simple atmospheric correction was applied using the modified blackbody method of Chavez (1988).

To a first approximation, the surface of these tropical glaciers can be modeled as a three component mixture of high reflectance snow and firn, lower reflectance dirty ice, and shade. A spectral library representing these three components as well as a local rock/soil endmember was constructed from a portion of the Landsat TM scene path 001 row 71 containing Zongo Glacier (**Figure 4.1**). Because of saturation of the TM sensor over snow covered surfaces, especially on northeast slopes that face directly into the sun, two endmembers were used to represent the accumulation zone. One endmember was selected to represent saturated pixels; the other to represent unsaturated pixels.

Figure 4.1: Endmember spectra used in the spectral mixture analysis



Ideally, laboratory or field spectra would be employed as the endmembers rather than values selected from the image itself. However, published high-resolution glacier spectra (Hall *et al.*, 1990; Hall *et al.*, 1989) seldom extend beyond the near infrared (1.1 to 1.2 μm) so comparison with at-satellite reflectances in Landsat bands 5 (1.55-1.75 μm) and 7(2.08-2.35 μm) was impossible. In the shorter visible and near-infrared wavelengths where published spectra do exist, the Landsat TM sensors were commonly saturated.

The six visible to mid-infrared bands of the Landsat images were used in the spectral mixture analysis with the endmembers described above plus a pure shade endmember. The pure shade endmember was included to account for differences in reflectance due to slope orientations and shadows. This was necessary as the endmembers were selected from the best illuminated areas on the glaciers.

Tropical Glaciers of Peru and Bolivia

The Andes of Peru and Bolivia contain approximately 90% of the glaciated area in the tropics (Jordan, 1991). This region is important in the study of tropical glaciers because they represent sources of water for hydroelectricity, irrigation, drinking, as well as recreation (Jordan, 1983). Two areas were chosen to illustrate the application of spectral mixing analysis to these tropical glaciers: Zongo Glacier in the Cordillera Real of Bolivia and the Quelccaya Ice Cap in Peru (**Figure 4.2**).

Figure 4.2: Landsat Thematic Mapper band 4 image of the central Andes, showing the locations of Zongo Glacier and the Quelccaya Ice Cap.

Zongo Glacier is a valley glacier located at 16°S, 68°W latitude on the Huayna Potosí massif approximately 40 northeast of the city of La Paz. Its elevation ranges from 4890 to 6000 m with its upper portions having a southerly orientation and its lower reaches an easterly exposure (Francou *et al.*, 1995). Since 1991, Zongo Glacier has been the site of ongoing glaciological investigations (Francou *et al.*, 1995; Ribstein *et al.*, 1995) and it offers the opportunity to correlate remote sensing observations of transient snowline with a mass balance time series. In contrast, Quelccaya is a small ice cap located in the eastern cordillera of Peru at 13° 56'S, 70° 50'W. Its surface area is 55 km² and it is 3-5 km in width and up to 17 km in length. The summit is located at approximately 5650 m with outlet glaciers extending down to 4900-5000 m (Thompson, 1980). Quelccaya has been the site of numerous glaciological studies over the past twenty years (e.g. Hastenrath, 1978; Thompson, 1980; Thompson, 1985; Thompson and Hastenrath, 1979; Thompson and Mosley-Thompson, 1987).

These tropical glaciers vary from their better studied mid-latitude counterparts in several important respects that must be considered when using visible and near- to mid-infrared images. Unlike temperate glaciers, the ablation and accumulation seasons of glaciers in the Peruvian-Bolivian Andes coincide and generally extend from October-May (Francou *et al.*, 1995). The period from June through early October is marked by dry and relatively cloud free conditions making it possible to follow the rise in transient snowline to its highest elevation. However, there is considerable

inter-annual variability in the mass balance and in the altitude of the equilibrium line (Francou *et al.*, 1995). Snowfall can also occur in the dry season. Therefore care must be taken when making any inference based on limited sampling of transient snowline positions.

The temperature regime of the tropics is dominated by a strong diurnal cycle. Temperatures in the afternoon even at elevations up to 4800 m are seldom below freezing (Johnson, 1976). High afternoon temperatures combined with intense shortwave radiation quickly melts snowcover falling outside of glaciers and perennial snow patches (Ribstein *et al.*, 1995) allowing glacier area to be estimated accurately.

Both field studies and analysis of Landsat TM and MSS images shows the surface character of the glaciers to be quite simple. The accumulation zone is commonly characterized by uniform high reflectance snow or firn whereas the ablation zone is typically bare ice with small patches of snow or firn (**Figure 4.3**). Variable amounts of rock debris and water also occur on the glacier surface, primarily within the ablation zone, but usually are minor components. Ice falls and cliffs produce shading at subpixel levels. Shadowing due to obscuring topography is also common.

Zongo

Zongo glacier is the best location in the central Andes for validation of spectral mixture analysis because it is the site of ongoing mass balance studies that can be used to compare transient snowline elevations to known

Figure 4.3: Field views of Zongo Glacier: **(a)** accumulation zone, **(b)** upper ablation zone, lower accumulation zone and terminus **(c)**. Ground photographs taken on August 8 and 9, 1994.

ELAs. As can be seen in the TM color composite (**Figure 4.4a**), two distinct zones appear on Zongo. These correspond well to the accumulation and ablation areas observed in the field since the inception of the glacier monitoring program in 1991.

The portion of the Landsat scene containing Zongo Glacier was spectrally unmixed using the endmembers shown in **Figure 4.1**. The resulting fractional abundance images which indicate the percentage of each endmember in a pixel are shown in **Figures 4.4b-4.4d**. The fractional abundance images of the two accumulation endmembers were summed to produce a single accumulation fractional abundance image. Comparison of **Figures 4.4b** and **4.4c** clearly show the ability of spectral mixture analysis to distinguish the accumulation and ablation zones on Zongo Glacier. Above the transient snowline (see **Figure 4.4a**), the fractional abundance of the accumulation endmembers is high (**Figure 4.4b**), whereas below the transient snowline the ablation endmember dominates (**Figure 4.4c**).

Shade (**Figure 4.4d**) is a small component over much of the glacier's surface. The uniform shade fraction found over most of the accumulation zone may be due in part to selection of endmembers from the best illuminated areas. The patches of high shade fraction below the transient snowline appear to correspond to several large ice falls in the lower reaches of the glacier. Overall, the RMS errors (**Figure 4.4f**) are quite low over much of Zongo glacier. The slightly higher RMS errors associated with the ablation zone may be due in part to inadequate selection of an ablation endmember,

Figure 4.4: (a) Landsat Thematic Mapper color composite of Zongo glacier, (b) accumulation zone fraction image, (c) ablation zone fraction image, (d) shade fraction image, (e) soil/rock fraction image, and (f) spectral mixture analysis RMS error

but are also consistent with the more heterogeneous nature of the ablation zone.

Spectral mixing also does an excellent job of discriminating between ice and snow and soil/rock. The glacier boundaries seen in the soil/rock endmember image (**Figure 4.4e**) agree well with the snow and ice covered areas determined using a binary snowcover classification (**Figure 4.5**) developed by Dozier (1989). The classification criterion for determination of snow and glacier covered pixels was as follows: reflectance in TM1 (0.45-0.52 μm) greater than 15%; reflectance in TM5 (1.55-1.75 μm) less than 15%; and the normalized difference ratio between TM2 (0.52-0.60 μm) and TM5, $[(\text{TM2}-\text{TM5})/(\text{TM2}+\text{TM5})]$, greater than 0.50. Because tropical glaciers cover only a small fraction of the landscape, the efficiency of the spectral mixing approach can be improved greatly by using a computationally frugal snow cover classification algorithm, such as that of (Dozier, 1989) or SNOMAP (Hall *et al.*, 1995b), to mask out unwanted pixels before spectral mixture analysis is performed.

Spectral mixing analysis of tropical glaciers is not without problems. Deep shadows present problems to any classification technique and spectral unmixing is no exception. The heavily shadowed areas in the accumulation area of Zongo glacier visible in the false color composite are characterized by a high fractional abundance of the ablation endmember (**Figure 4.4c**) rather than a mix of accumulation and shade. The problem is not limited to spectral

Figure 4.5: Binary snow cover classification of Zongo Glacier

mixture analysis as snow was mapped incorrectly over many of the heavily shadowed areas by the simpler binary classifiers as well (**Figure 4.5**).

The transient snowline can be easily identified on Zongo glacier using spectral mixing analysis, despite inadequate knowledge of the number and character of image endmembers. The elevation of the transient snowline is easily determined by plotting the accumulation and ablation endmembers fractions along a transect across the glacier (**Figure 4.6**). At the transient snowline there is an abrupt shift in both accumulation and ablation endmember fractions. Comparison of the fractional abundance images with a TM4/TM5 ratio (**Figure 4.7**), clearly shows the superiority of the spectral mixture analysis to band ratios in identification of the transient snowline. The transient snowline clearly visible in the endmember fraction images is difficult or impossible to discern on the ratio image.

The elevation of the transient snowline at the time the TM image was acquired was 5120 m. Although the transient snowline may not have reached its highest elevation by early August, this elevation compares well to later ELA estimates made using a traditional stake network. During 1991-1992, the equilibrium line was at 5300 m and during 1992-1993 it was at 5100 m. The difference in the ELA between the two balance years was caused by an ENSO event during 1991-1992. In this portion of the Andes, ENSO events are marked by dry, hot, and sunny conditions that cause the ELA to rise much higher than under more normal conditions, such as during 1992-1993 in which the net balance was nearly zero (Francou *et al.*, 1995).

Figure 4.6: (a) Fractional endmember abundances versus elevation along a transect across Zongo glacier shown in **Figure 4.4a**. and (b) fractional endmember abundances and elevations versus distance along the same transect.

Figure 4.7: Landsat TM4/TM5 band ratio of Zongo glacier

The highest elevation the transient snowline reached during the 1986-1987 balance year is unknown, but by early August, the transient snowline had already reached the height of the ELA for an equilibrium year. This strongly suggests that the net balance of Zongo Glacier for 1986-1987 hydrologic year was negative. This agrees well with the temperature and precipitation records of El Alto/La Paz and the occurrence of a ENSO event during this period.

Quelccaya

Spectral unmixing was also performed over an area containing the Quelccaya Ice Cap to examine the portability of spectral endmembers from one area in the central Andes to another. Visual examination of the Landsat TM color composite of Quelccaya (**Figure 4.8a**) suggests that, like Zongo, two distinct spectral zones exist on the ice cap and outlet glaciers. Additionally, the strong contrast between the ice cap and surrounding area suggest that spectral mixing should allow good delineation of the ice cap margins. The spectral mixture analysis was undertaken using the endmembers selected from Zongo Glacier.

Even though the spectral endmembers were selected from a different area, the results of spectral mixing are quite remarkable. Like at Zongo, the soil/bedrock fraction image clearly discriminates between glacier and non glacial areas (**Figure 4.8b**). The accumulation (**Figure 4.8c**) and ablation (**Figure 4.8d**) zones are easily distinguished in the fraction images.

Figure 4.8: (a) Landsat Thematic Mapper color composite of the Quelccaya (b) soil/rock fraction image, (c) accumulation zone fraction image, (d) ablation fraction image, (e) shade fraction image, and (f) RMS errors

In particular, the ablation areas which are located on a series of small outlet glaciers are clearly visible in the ablation fraction image are less well differentiated in the TM4/TM5 ratio image (**Figure 4.9**). Subtle ice cap topography is revealed in both the accumulation and shade (**Figure 4.8e**) fraction images. Like in the Zongo image RMS errors (**Figure 4.8f**) are low and the highest errors correspond to valley bottoms where vegetation is present. This is to be expected as vegetation was not included in the analysis. On the ice cap itself, the pattern of RMS errors corresponds to topographic variations. A simple linear combination of an accumulation area endmember, in which several of the TM bands are saturated, and shade cannot perfectly model the observed variations in at-satellite reflectances of this high albedo surface. It is interesting, and encouraging, to note that on many outlet glaciers shade is a very small component. Thus ablation areas were correctly identified, and not misidentified as topographically shaded accumulation areas, which they can resemble on Landsat TM false color composites.

Summary

Spectral mixture analysis of Landsat Thematic Mapper images has been found to be an ideal technique for delineating the accumulation and ablation zones on tropical glaciers and provides a tool to accurately map the transient snowline. Delineation of the accumulation and ablation zones is robust and quite insensitive to the exact endmembers employed. It appears

Figure 4.9: Landsat TM4/TM5 band ratio of the Quelccaya Ice Cap.

possible to transfer a spectral library developed on one glacier to another area, which is important because surface conditions are monitored on few glaciers in the region. Spectral mixing is found to be superior to either single bands or band ratios in detection of the transient snowline. As visible and near to mid-infrared images become available at better spatial resolution, remote sensing and spectral mixing analysis will become a more viable option for the study of tropical glaciers.

Bibliography

- Adams, J. B., and Smith, M. O. (1986). Spectral mixing modeling: a new analysis of rock and soil types at the Viking 1 Lander site. *Journal of Geophysical Research* **91**, 8098-8112.
- Bayr, K. J., Hall, D. K., and Kovalick, W. M. (1994). Observations on glaciers in the eastern Austrian Alps using satellite data. *International Journal of Remote Sensing* **15**, 1733-1742.
- Boardman, J. W. (1990). Inversion of imaging spectrometry data using singular value decomposition. In "IGARSS.", pp. 1036-1039.
- Chavez, P. S. (1988). An improved dark-object subtraction technique for atmospheric scattering correction of multispectral data. *Remote Sensing of Environment* **24**, 459-479.
- Dozier, J. (1989). Spectral signature of alpine snow cover from the Landsat Thematic Mapper. *Remote Sensing of Environment* **28**, 9-22.
- Francou, B., Ribstein, P., Saravia, R., and Tiriau, E. (1995). Monthly balance and water discharge of an inter-tropical glacier: Zongo Glacier, Cordillera Real, Bolivia, 16° S. *Journal of Glaciology* **41**, 61-67.
- Hall, D. K., Benson, C. S., and Field, W. O. (1995a). Changes of glaciers in Glacier Bay, Alaska, using ground and satellite measurements. *Physical Geography* **16**, 27-41.
- Hall, D. K., Binschadler, R. A., Foster, J. L., Chang, A. T. C., and Siddalingaiah, H. (1990). Comparison of *in situ* and satellite-derived reflectances of Forbindels Glacier, Greenland. *International Journal of Remote Sensing* **11**, 493-504.
- Hall, D. K., Chang, A. T. C., Foster, J. L., Benson, C. S., and Kovalick, W. M. (1989). Comparison of In Situ and Landsat derived reflectance of Alaskan glaciers. *Remote Sensing of Environment* **28**, 23-31.
- Hall, D. K., Ormsby, J. P., Bindschadler, R. A., and Siddalingaiah, H. (1987). Characterization of snow and ice reflectance zones on glaciers using Landsat Thematic Mapper Data. *Annals of Glaciology* **9**, 104-108.

- Hall, D. K., Riggs, G. A., and Salomonson, V. V. (1995b). Development of methods for mapping global snow cover using moderate resolution imaging spectroradiometer data. *Remote Sensing of Environment* **54**, 127-140.
- Hastenrath, S. (1978). Heat-budget measurements on the Quelccaya Ice Cap, Peruvian Andes. *Journal of Glaciology* **20**, 85-97.
- Hastenrath, S. (1984a). "The Glaciers of Equatorial East Africa." D. Reidel Publishing Company, Dordrecht, Holland.
- Hastenrath, S. (1989). Ice flow and mass changes of Lewis Glacier, Mount Kenya, Kenya, East Africa: observations 1974-86, modeling, and predictions to the year 2000 A.D. *Journal of Glaciology* **35**, 325-332.
- Hastenrath, S., and Ames, A. (1995). Diagnosing the imbalance of the Yanamarey Glacier in the Cordillera Blanca of Peru. *Journal of Geophysical Research* **100**, 5105-5112.
- Hastenrath, S., and Kruss, P. D. (1992a). The dramatic retreat of Mount Kenya's glaciers between 1963 and 1987: greenhouse forcing. *Annals of Glaciology* **16**, 127-133.
- Hastenrath, S., and Kruss, P. D. (1992b). Greenhouse Indicators in Kenya. *Nature* **355**, 503-504.
- Hastenrath, S. L. (1984b). Tropical glacier and climate variations. *Endwissenschaftliche Forschung* **18**, 235-248.
- Hope, G. S., Peterson, J. A., Radok, U., and Allison, I. (1976). "The Equatorial Glaciers of New Guinea." A.A. Balkema, Rotterdam.
- Johnson, A. M. (1976). The climate of Peru, Bolivia, and Ecuador. In "The Climate of South America." (W. Schwerdtfeger, Ed.), pp. 147-218. World Survey of Climatology. Elsevier Scientific Publishing Company, Amsterdam-Oxford-New York.
- Jordan, E. (1983). The Utility of a Glacier Inventory to Developing Countries such as Bolivia. . *Quaternary of South America and Antarctic Peninsula* **1**, 125-134.
- Jordan, E. (1991). "Die Gletscher der bolivianischen Andean." Franz Steiner Verlag Stuttgart, Eurasburg, Germany.

- Kaser, G., Ames, A., and Zamora, M. (1990). Glacier fluctuations and climate in the Cordillera Blanca, Peru. *Annals of Glaciology* **14**, 136-140.
- Kerr, A. (1993). Topography, climate and ice masses: a review. *Terra Nova* **5**, 332-342.
- Krimmel, R. M., and Meier, M. F. (1975). Glacier applications of ERTS images. *Journal of Glaciology* **15**, 493-504.
- Markham, B. L., and Barker, J. L. (1986). Landsat MSS and TM post-calibration dynamic ranges, exoatmospheric reflectances and at satellite temperatures. *EOSAT Technical Notes* **1**, 3-8.
- Meier, M. F. (1973). Evaluation of ERST imagery for mapping and detection of changes in snowcover on land and on glaciers. In "Symposium on Significant Results Obtained from the Earth Resources Technology Satellite-1.", pp. 863-875. NASA SP-327, Washington, D.C.
- Ø strem, G. (1975). ERTS data in glaciology -- an effort to monitor glacier mass balance from satellite imagery. *Journal of Glaciology* **15**, 403-415.
- Paterson, W. S. B. (1994). "The Physics of Glaciers." Elsevier Science Ltd., Oxford.
- Press, W. H., Flannery, B. P., Teukolsky, S. A., and Vetterling, W. T. (1988). "Numerical Recipes in C." Cambridge University Press, Cambridge.
- Ribstein, P., Tiriau, E., Francou, B., and Saravia, R. (1995). Tropical climate and glacier hydrology: a case study in Bolivia. *Journal of Hydrology* **165**, 221-234.
- Rosenthal, W., and Dozier, J. (1996). Automated mapping of montane snow cover at subpixel resolution from the Landsat Thematic Mapper. *Water Resources Research* **32**, 115-130.
- Sabol, D. E., Adams, J. B., and Smith, M. (1990). Predicting the Spectral Detectability of Surface Materials Using Spectral Mixture Analysis. In "IGARSS'90.", pp. 967 - 970.
- Thompson, L. G. (1980). Glaciological investigations of the tropical Quelccaya Ice Cap, Peru. *Journal of Glaciology* **25**, 69-84.

- Thompson, L. G. (1985). A 1500-year record of tropical precipitation in ice cores from the Quelccaya Ice Cap, Peru. *Science* **229**, 971-973.
- Thompson, L. G., and Hastenrath, S. (1979). Climatic ice core records from the tropical Quelccaya Ice Cap. *Science* **203**, 1240-1243.
- Thompson, L. G., and Mosley-Thompson, E. (1987). Evidence of Abrupt Climatic Change during the Last 1500 Years Recorded in Ice Cores from the Tropical Quelccaya Ice Cap, Peru. *Abrupt Climatic Change*, 99-110.
- van Ufford, A. Q., and Sedgwick, P. (submitted). Recession of the equatorial Puncak Jaya glaciers (1825-1995), Irian Jaya (western New Guinea), Indonesia. *submitted to Geology*.
- Williams, R. S. J., Hall, D. K., and Benson, C. S. (1991). Analysis of glacier facies using satellite techniques. *Journal of Glaciology*, 120-128.